PHYSICAL REVIEW A, VOLUME 62, 042503

Molecular deformation in the O $1s^{-1}2\pi_u$ excited states of CO_2 probed by the triple-differential measurement of fragment ions

N. Saito,[1] K. Ueda,[2] M. Simon,[2,3,4] K. Okada,[5] Y. Shimizu,[2] H. Chiba,[2] Y. Senba,[6] H. Okumura,[7] H. Ohashi,[8] Y. Tamenori,[8] S. Nagaoka,[9] A. Hiraya,[6] H. Yoshida,[6] E. Ishiguro,[10] T. Ibuki,[11] I. H. Suzuki,[1] and I. Koyano[7]

[1]*Electrotechnical Laboratory, Tsukuba 305-8568, Japan*

[2]*Research Institute for Scientific Measurements, Tohoku University, Sendai 980-8577, Japan*

[3]*LURE, Batiment 209d, Universite Paris-Sud, 91405 Orsay Cedex, France*

[4]*CEA/DRECAM/SPAM, CEN Saclay, 91191 Gif-Yvette Cedex, France*

[5]*Department of Chemistry, Hiroshima University, Higashi-Hiroshima 739-8526, Japan*

[6]*Department of Physical Sciences, Hiroshima University, Higashi-Hiroshima 739-8526, Japan*

[7]*Department of Material Science, Himeji Institute of Technology, Kamigori, Hyogo 678-1297, Japan*

[8]*Japan Synchrotron Radiation Research Institute, Sayo-gun, Hyogo 679-5198, Japan*

[9]*Institute for Molecular Science, Okazaki 444-8585, Japan*

[10]*College of Education, University of the Ryukyus, Nishihara-cho, Okinawa 903-0213, Japan*

[11]*Kyoto University of Education, Fushimi-ku, Kyoto 612-8522, Japan*

(Received 7 March 2000; published 11 September 2000)

Measurement of mass-, energy-, and angle-resolved fragment ions reveals that the β value for C^+ with kinetic energy $\geqslant 3$ eV is ~ 0.9 in the region of the O $1s \rightarrow 2\pi_u$ excitation and that the β value for O^+ with kinetic energy $\geqslant 4$ eV varies from -0.23 to -0.57 across the O $1s \rightarrow 2\pi_u$ resonance. These findings postulate that the CO_2 molecule excited to the lower branch of the vibronically split O $1s^{-1}2\pi_u$ excited states deforms into a bent geometry while the molecule excited to the higher branch remains in a linear geometry.

PACS number(s): 33.20.Rm, 33.20.Wr, 33.15.Bh

I. INTRODUCTION

Recent developments of synchrotron radiation sources and soft-x-ray monochromators invoked renewal of interests in the photoabsorption spectroscopy of free molecules in the core-excitation region. One can now observe the detailed structures in the spectra with the photon bandpass narrower than the core-hole lifetime width and analyze them to extract the information of the nuclear motion and the vibronic coupling in the core-excited states (see, for example, [1–4]).

Angular distribution measurements of fragment ions from a core-excited molecule, on the other hand, provide additional information such as the symmetry and molecular deformation in core-excited states [5–22]. Time scales of core-hole decay and subsequent dissociation are of an order of $10^{-14}-10^{-13}$ s and thus much shorter than time scales of $10^{-12}-10^{-11}$ s of the molecular rotation. Thus, for $\Sigma \rightarrow \Sigma$ and $\Sigma \rightarrow \Pi$ transitions in diatomic molecules, the fragment ions energetically ejected are preferentially detected in the direction parallel and perpendicular, respectively, to the polarization vector of the incident light (hereafter referred to as the *E* vector). Therefore, one can determine the symmetries of core-excited states from the angular distribution measurements of fragment ions [5–11].

With polyatomic molecules, however, the angular distributions of fragment ions do not always reflect the symmetries of core-excited electronic states because of the complex vibronic coupling effects in the core-excited states [14–21]. In CO_2, for example, the core-excited C $1s^{-1}2\pi_u$ states, which are originally degenerated, are split into two states via the vibronic coupling with the bending vibration. The lower one in energy has a bent stable geometry while the higher one has a linear stable geometry. As a result, the fragments from the lower-energy state can be ejected with a non-negligible velocity component perpendicular to the molecular axis [18–20].

In the present paper, we demonstrate that a method for the measurement of the mass-, energy-, and angle-resolved fragment ions (i.e., triple-differential measurement), combined with a narrow bandpass monochromatic soft-x-ray excitation source, is a powerful tool to investigate the molecular deformation in the core-excited states of polyatomic molecules. For this purpose, we focus on the O $1s \rightarrow 2\pi_u$ excitation. The excitation spectrum in the range of interest was investigated by Refs. [23,24] and we follow the assignments they presented. Cesar *et al.* [25] investigated the soft-x-ray emission both experimentally and theoretically in the vicinity of the O $1s\sigma_g \rightarrow 2\pi_u$ excitation. Their interest was the symmetry breaking due to the vibronic coupling between O $1s\sigma_g \rightarrow 2\pi_u$ and O $1s\sigma_u \rightarrow 2\pi_u$ with the antisymmetric stretching vibration (Σ_u) and its excitation energy dependence. In the theoretical treatment by Cesar *et al.*, they neglected other vibronic couplings such as Renner-Teller coupling within the degenerate O $1s^{-1}2\pi_u$ states and quasi-Jahn-Teller [26,27] coupling between O $1s^{-1}2\pi_u$ and the closely lying O $1s^{-1}3s\sigma_g$ state with the bending vibration (Π_u). The vibronic coupling with the bending vibration and the molecular deformation due to the vibronic coupling are of our current interest.

II. EXPERIMENT

The experiments are performed using a high-resolution plane grating monochromator [28] installed on the *c* branch of the soft-x-ray figure-8 undulator beamline 27SU at

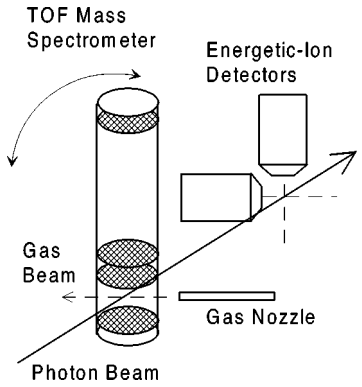

FIG. 1. Schematic diagram of the experimental setup. The TOF mass spectrometer and the pair of energetic-ion detectors are placed in tandem along the incident photon beam, the former sitting upstream of the latter. The TOF mass spectrometer and its gas nozzle can be rotated from $-20°$ to $110°$ with respect to the horizontal position.

SPring-8 [29,30]. This beamline provides linearly polarized monochromatic soft x rays. The photon bandpass is set to ~ 55 meV at ~ 535 eV in the present experiment. The direction of the E vector for the first-order harmonic photon is horizontal whereas that of the 0.5th-order harmonic photon is vertical. Thus the direction of the E vector can be switched from horizontal to vertical and vice versa by simply varying the gap of the undulator.

Figure 1 shows a schematic diagram of the experimental setup [31,32]. Two types of analyzer are used in the present study: a linear time-of-flight (TOF) mass spectrometer with a 690 mm long drift tube and a pair of energetic-ion detectors. These are mounted on a rotatable ultrahigh-vacuum chamber in tandem, the former being placed upstream of the latter along the incident photon beam and 250 mm apart from each other. The collected electrons and ions are detected by microsphere plates (MSPs). An effusive molecular beam of CO_2 from a gas nozzle is crossed with the photon beam at a point just in front of the entrance to the TOF mass spectrometer and lying on the drift tube axis. The TOF mass spectrometer together with the gas nozzle can be rotated around the photon beam through an angle between $-20°$ and $110°$ from the horizontal position. The energetic-ion detectors are of the retarding-field type and one is mounted horizontally and the other vertically. These again can be rotated around the photon beam axis, but independently of the rotation of the TOF mass spectrometer. A molecular beam of CO_2 for the latter detectors is introduced coaxially with the photon beam using another gas nozzle (not shown in Fig. 1).

Triple-differential (i.e., mass-, energy-, and angle-resolved) measurements for fragment ions are carried out at several photon energies within the O $1s \rightarrow 2\pi_u$ resonance, using the TOF mass spectrometer. The spectrometer is operated under a McLaren space focusing condition with an extraction field of 200 V/cm. The gas pressure is adjusted between 3×10^{-4} and 6×10^{-3} Pa in the experimental chamber to obtain a constant count rate of the ions. The TOF mass spectra are measured at $0°$, $55°$, and $90°$ with respect to the E vector of the incident photon. To achieve this, the

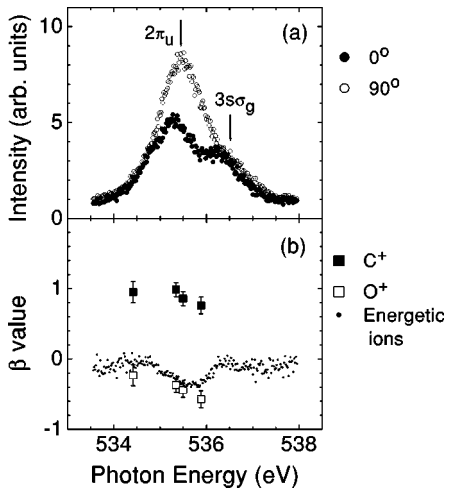

FIG. 2. Yield spectra and asymmetry parameters of fragment ions from CO_2 in the O $1s^{-1}2\pi_u$ excited states. (a) Angle-resolved energetic photoion-yield spectra. Solid circles denote the ion yield at $0°$ and open circles at $90°$. (b) The asymmetry parameter (β) values of the energetic C^+ (solid squares), energetic O^+ (open squares), and energetic nonspecified ions (dots).

TOF axis is first set in the vertical direction and measurements are taken using both the first-order (horizontal polarization) and 0.5th-order (vertical polarization) photons. Then the spectrometer axis is set in the $55°$ direction and measurements are taken using the first-order photons. It has been confirmed from the photoelectron spectra of Ne $2s$ and $2p$ measured using an electron energy analyzer (not shown in Fig. 1) that the degrees of the polarization are $>98\%$ for both horizontal and vertical polarization. The signals from the electron MSP were used as a start signal to obtain the TOF mass spectra.

The measurements of yield curves for the energetic ions (masses not separated) are performed using the pair of energetic-ion detectors. The direction of the E vector of the incident photons is switched horizontally and vertically by varying the gap of the undulator, as mentioned above. Thus each detector at the fixed position measures energetic ions emitted in the direction parallel to the E vector at one time and those emitted perpendicularly to the E vector at another time. In this way the energetic-ion yield spectra $I(0°)$ and $I(90°)$ compensated for the difference in the detection efficiency of the two detectors are directly obtained. The retarding voltage used is 5 V and thus the ions detected are those with kinetic energies higher than 5 eV. These spectra are combined with the results of the high-resolution TOF measurements to deduce values of the asymmetry parameter β for each of the mass-selected fragment ions C^+ and O^+ as a function of the photon energy.

III. RESULTS

Figure 2(a) shows the yield spectra $I(0°)$ and $I(90°)$ of the energetic photoions ($\geqslant 5$ eV) measured at $0°$ and $90°$. Similar spectra have been observed quite recently also by Adachi *et al.* [33]. Peaks at ~ 535.4 eV mainly correspond to the O $1s \rightarrow 2\pi_u$ excitation. (The photon energy was cali-

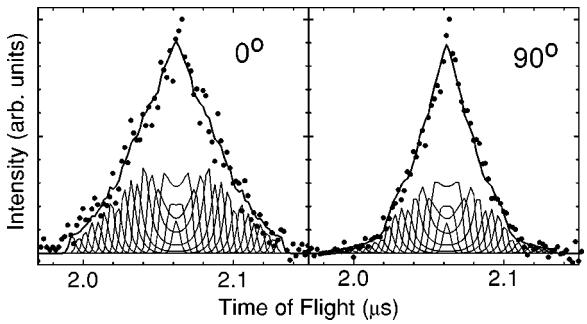

FIG. 3. TOF spectra (dots) of C^+ ions at the photon energy of 535.35 eV recorded at 0° and 90° with respect to the *E* vector. The TOF spectra at the energy of 530.6 eV are subtracted. The narrow curves denote the calculated TOF spectra for the kinetic energies of 0.01–8 eV and the β values of 0.11 (0.01–0.8 eV), 0.35 (0.8–3 eV), and 0.99 (3–8 eV). The thick curves are the sum of the narrow curves and are fitted to the experimental spectra.

brated so that the peak energy observed in the total ion-yield spectrum, not shown here, agrees with the literature value 535.4 eV [34].) The peak at 536.4 eV of the $I(0°)$ spectrum is attributed to the O $1s \rightarrow 3s\sigma_g$ excitation [23,24,34]: this peak appears as a weak shoulder in the $I(90°)$ spectrum.

The angular distribution of the fragment ions relative to the *E* vector can be described by

$$I(\theta) = C[1 + \beta P_2(\theta)], \tag{1}$$

where θ is the angle between the *E* vector and the direction of the ion detection, β is the asymmetry parameter, P_2 is the Legendre second-order polynomial, and *C* is a scaling factor proportional to the cross section. From Eq. (1) we have a relation between β and the measured quantities $I(0°)$ and $I(90°)$:

$$\beta = \frac{2[I(0°) - I(90°)]}{I(0°) + 2I(90°)}. \tag{2}$$

The values of β obtained using Eq. (2) are plotted in Fig. 2(b).

In the energetic-ion yield measurements described above, the detected ions can be a mixture of different ions and different ions can have different β values. The β values for energy-selected C^+ and O^+ ions were extracted from the high-resolution TOF spectra, such as those given in Fig. 3, in the following manner. First, in order to remove the contributions from valence ionization and C 1*s* ionization to the β values, we subtracted the TOF spectrum recorded at the energy of 530.6 eV, far from the resonance, from the TOF spectra recorded at several photon energies within the O $1s \rightarrow 2\pi_u$ resonance. Then we fitted the peak shapes for C^+ and O^+ in the spectra to the model described in detail previously [5,14,18] and obtained the kinetic energy distributions for C^+ and O^+. Note that the β value can be dependent on the ion kinetic energy. Thus, in order to obtain the energy-dependent β values, we divided the kinetic-energy distributions for C^+ and O^+ into three ranges, say, low-, medium-, and high-energy ranges: these divisions were somehow arbitrary. We finally obtained the β values for each energy range of C^+ and O^+ from the data set recorded at 0°, 55°, and 90° with respect to the *E* vector. The β values of C^+ and O^+ at the excitation energy far from the resonance (530.63 eV, not shown in the Fig. 2) were ~ 0 for all kinetic energy ranges.

We are particularly interested in the angular distribution of high-energy ions, i.e., $\geqslant 3$ eV for C^+ and $\geqslant 4$ eV for O^+ in the present analysis, because the rotation motion of molecules can be neglected for dissociation with higher kinetic energy release. The energetic ($\geqslant 5$ eV) O^+ was produced about six times as much as energetic ($\geqslant 5$ eV) C^+. Thus the energetic ($\geqslant 5$ eV) ions detected in the ion-yield measurement in Fig. 2(a) were mostly the O^+ ions. The resulting values of β for O^+ ($\geqslant 4$ eV) are plotted in Fig. 2(b) with open squares and compared with the β values obtained from the energetic ion-yield curve. The behavior of the β value for O^+ is similar to (though slightly lower than) those obtained from the energetic ion yield curve. The β values of the energetic ($\geqslant 3$ eV) C^+ ions are plotted also in Fig. 2(b) with solid squares.

IV. DISCUSSION

To interpret the angular distributions of fragment ions described above, it is important to know stable geometries in core-excited states because the molecular deformation in the core-excited state often affects the angular distribution of the fragment ions. The core-excited states involved here are the twofold degenerate O $1s^{-1}2\pi_u$ and O $1s^{-1}3s\sigma_g$ ones. We consider the vibronic couplings with the bending vibration of Π_u symmetry, i.e., Renner-Teller coupling within the degenerate O $1s^{-1}2\pi_u$ states and quasi-Jahn-Teller coupling between O $1s^{-1}2\pi_u$ and O $1s^{-1}3s\sigma_g$. This multistate Σ-Π coupling model is fully discussed in [27]. Then, the O $1s^{-1}2\pi_u$ states are split into two states and the lower one in energy is expected to have a bent geometry. This state can be denoted as in-plane O $1s^{-1}2\pi_u$ because the π orbital lies in the plane of the bent geometry [19,20]. The upper state originating from O $1s^{-1}2\pi_u$ has a linear geometry: this state can be denoted as out-of-plane O $1s^{-1}2\pi_u$ because the π orbital is perpendicular to the plane of the bent geometry [19,20]. The above described molecular deformation caused by the vibronic coupling with the bending vibration can be confirmed with the help of the equivalent core model. In this model, the in-plane O $1s^{-1}2\pi_u$ excited state can be approximated by the ground state of FCO whose stable geometry is indeed known to be bent: r(C-F)=1.334 Å$_3$ r(C-O) =1.169 Å , and $\theta_{\text{F-C-O}}$=127.3° [35].

Note that we can expect that the $1s^{-1}3s\sigma_g$ state has a linear stable geometry. We will discuss the effect of the above Σ-Π vibronic coupling onto the $1s^{-1}3s\sigma_g$ state later.

In the above consideration of the vibronic coupling, we neglected the vibronic couplings (quasi-Jahn-Teller coupling) between O $1s\sigma_g^{-1}3s\sigma_g$ Σ_g and O $1s\sigma_u^{-1}3s\sigma_g$ Σ_u

and between O $1s\sigma_g^{-1}2\pi_u$ Π_u and O $1s\sigma_u^{-1}2\pi_u$ Π_g with the antisymmetric vibration (Σ_u) for simplicity. These couplings induce *g-u* symmetry breaking, as discussed by Cesar *et al.* [25], but do not affect the angular distributions of the fragment ions.

Under the axial-recoil approximation where one neglects the effect of the molecular rotations on the dissociation, we can express the β value for the fragment ions in terms of the angle χ between the dipole moment μ and the direction of detection of the fragment [36–38]:

$$\beta = 2P_2(\cos\chi). \tag{3}$$

In the case of the $\Sigma_g \rightarrow \Sigma_u$ and $\Sigma_g \rightarrow \Pi_u$ transitions, μ is parallel and perpendicular to the O-C-O molecular axis, respectively. Therefore, if the fragment ions (mostly O^+) are ejected along the molecular axis, $\chi = 0°$ and thus $\beta_\Sigma = 2$ for $\Sigma_g \rightarrow \Sigma_u$ and $\chi = 90°$ and thus $\beta_\Pi = -1$ for $\Sigma_g \rightarrow \Pi_u$.

If both the $\Sigma_g \rightarrow \Sigma_u$ and $\Sigma_g \rightarrow \Pi_u$ transitions overlap, say, in the continua, the β value can be given by the weighted average of these two transition components:

$$\beta = \frac{\sigma_\Sigma \beta_\Sigma + \sigma_\Pi \beta_\Pi}{\sigma_\Sigma + \sigma_\Pi}, \tag{4}$$

where σ_Σ and σ_Π are partial cross sections for $\Sigma_g \rightarrow \Sigma_u$ and $\Sigma_g \rightarrow \Pi_u$, respectively. The measured β values were ~ 0 for O^+ for all kinetic energy ranges when the excitation energy was far from the resonance. The reason for this finding is that the ratio $\sigma_\Sigma : \sigma_\Pi$ can be well approximated by the statistical ratio 1:2.

Let us consider the β values for the energetic O^+ ions. The β value changes from -0.23 at the lower-energy foot (534.42 eV) of the O $1s \rightarrow 2\pi_u$ resonance to -0.57 at the higher-energy shoulder (535.89 eV) of the resonance, as shown in Fig. 2(b). The influence from the valence and C $1s$ excitations was subtracted and thus the measured β values directly reflect the fragmentation from the O $1s^{-1}2\pi_u$ states. If O^+ were ejected along the molecular axis, β_Π would be -1 for the pure $\Sigma_g \rightarrow \Pi_u$ transition. One possibility for the deviation of the β values from the expected value -1 is the contribution from the $\Sigma_g \rightarrow \Sigma_u$ transition induced by the quasi-Jahn-Teller coupling between O $1s\sigma_u^{-1}3s\sigma_g$ Σ_u and O $1s\sigma_u^{-1}2\pi_u$ Π_g with the bending vibration. If this is the case, the intensity at the O $1s^{-1}2\pi_u$ resonance in the $I(0°)$ spectrum of Fig. 2(a) should be smaller (e.g., 20% [39]) than that of the O $1s^{-1}3s\sigma_g$ resonance in $I(0°)$. Since the present result exhibits a higher intensity for the O $1s^{-1}2\pi_u$ resonance than the O $1s^{-1}3s\sigma_g$ resonance, this contribution is considered to be minor. The large deviation of the β values from -1 can be explained only as a result of molecular deformation to the bent geometry in the in-plane O $1s^{-1}2\pi_u$ state as discussed above.

Now we move to the β values for the energetic C^+ ions. The β values are ~ 0.9 in the region of the O $1s \rightarrow 2\pi_u$ resonance, as shown in Fig. 2(b). If C^+ were ejected along the molecular axis, β_Π would be -1. If C^+ were ejected in the direction perpendicular to the molecular axis, then both the dipole moment μ and the velocity vector of C^+ are within the $D_{\infty h}$ symmetry plane and χ can be arbitrary within this plane: in this case the expected β_Π value is 0.5 [21]. The values of β larger than 0.5 can be explained only by treating the in-plane and out-of-plane O $1s^{-1}2\pi_u$ states separately. If the O $1s$ electron is excited to the in-plane $2\pi_u$ orbital, we can expect that C^+ is ejected in the direction parallel to the in-plane $2\pi_u$ orbital because this is the direction of the bending motion excited in the core-excited state. In this case we expect $\beta_{\text{in}\,\Pi} = 2$. If the O $1s$ electron is excited to the out-of-plane $2\pi_u$ orbital, the direction of the bending motion is perpendicular to the out-of-plane $2\pi_u$ orbital, and C^+ is ejected to this direction. Then we expect $\beta_{\text{out}\,\Pi} = -1$. Thus the measured result of β values larger than 0.5 is direct evidence that the energetic C^+ is preferentially ejected from the in-plane O $1s^{-1}2\pi_u$ in the bent geometry, rather than from the out-of-plane O $1s^{-1}2\pi_u$ in the linear geometry.

Finally, we discuss the angular distributions of the energetic ions in the region of the O $1s \rightarrow 3s\sigma_g$ resonance. We expect that the O $1s^{-1}3s\sigma_g$ state has the linear stable geometry and the energetic ions are dominated by O^+ ejected along the molecular axis. Then, only the transition to O $1s\sigma_u^{-1}3s\sigma_g$ Σ_u would appear in $I(0°)$ and $\beta_\Sigma = 2$, if the vibronic couplings were negligible. As seen in Fig. 2, however, the $\Sigma_g \rightarrow \Pi_u$ transition in $I(90°)$ is as significant as the $\Sigma_g \rightarrow \Sigma_u$ transition in $I(0°)$. The $\Sigma_g \rightarrow \Pi_u$ transitions can appear as a result of the vibronic coupling with the bending vibration. Taking account of the vibronic couplings with the antisymmetric vibration as well, we can conclude that the $\Sigma_g \rightarrow \Sigma_u$ transition observed in $I(0°)$ includes the transitions to O $1s\sigma_u^{-1}3s\sigma_g$ $\Sigma_u \times (n,0,0)\Sigma_g : \Sigma_u$ and O $1s\sigma_g^{-1}3s\sigma_g$ $\Sigma_g \times (n,0,1)\Sigma_u : \Sigma_u$, whereas the $\Sigma_g \rightarrow \Pi_u$ transition observed in $I(90°)$ includes O $1s\sigma_g^{-1}3s\sigma_g$ $\Sigma_g \times (n,1,0)\Pi_u : \Pi_u$ and O $1s\sigma_u^{-1}3s\sigma_g$ $\Sigma_u \times (n,1,1)\Pi_g : \Pi_u$, where (v_1,v_2,v_3) and v_1, v_2, and v_3 are symmetric stretching, bending, and antisymmetric stretching vibrations. Because of the overlap of the symmetric and antisymmetric stretching vibrations, we cannot resolve the vibrational structure in the spectra of Fig. 2(a).

In conclusion, we reported the triple-differential measurements for the fragment ions and demonstrated that this method is a powerful tool to investigate the molecular deformation in core-excited states.

ACKNOWLEDGMENTS

This experiment was carried out with the approval of the SPring-8 program Advisory Committee (Proposal No. 1999B0290-NS-np) and supported in part by Grants-in-aid for Scientific Research from the Japanese Ministry of Education, Science, Sports and Culture and by the Matsuo Foundation. The authors are grateful to the staff of SPring-8 for their help in the course of the experiments.

[1] F. X. Gadea, H. Koppel, J. Schirmer, L. S. Cederbaum, K. J. Randall, A. M. Bradshaw, Y. Ma, F. Sette, and C. T. Chen, Phys. Rev. Lett. **66**, 883 (1991).
[2] G. Remmers, M. Domke, and G. Kaindl, Phys. Rev. A **47**, 3085 (1993).
[3] K. Ueda, M. Okunishi, H. Chiba, Y. Shimizu, K. Ohmori, Y. Sato, E. Shigemasa, and N. Kosugi, Chem. Phys. Lett. **236**, 311 (1995).
[4] S. Itoh, S. Tanaka, and Y. Kayanuma, Phys. Rev. A **60**, 4488 (1999).
[5] N. Saito and I. H. Suzuki, Phys. Rev. Lett. **61**, 2740 (1988); Int. J. Mass Spectrom. Ion Processes **82**, 61 (1988).
[6] A. Yagishita, H. Maezawa, M. Ukai, and E. Shigemasa, Phys. Rev. Lett. **62**, 36 (1989).
[7] K. Lee, D. Y. Kim, C. I. Ma, D. A. Lapiano-Smith, and D. M. Hanson, J. Chem. Phys. **93**, 7936 (1990).
[8] E. Shigemasa, K. Ueda, Y. Sato, T. Sasaki, and A. Yagishita, Phys. Rev. A **45**, 2915 (1992).
[9] O. Hemmers, F. Heiser, J. Eiben, R. Wehlitz, and U. Becker, Phys. Rev. Lett. **71**, 987 (1993).
[10] N. Saito, F. Heiser, O. Hemmers, K. Wieliczek, J. Viefhaus, and U. Becker, Phys. Rev. A **54**, 2004 (1996).
[11] K. Lee, D. Y. Kim, C. I. Ma, and D. M. Hanson, J. Chem. Phys. **100**, 8550 (1994).
[12] T. Lebrun, M. Lavollée, M. Simon, and P. Morin, J. Chem. Phys. **98**, 2534 (1993).
[13] M. Simon, M. Lavollée, M. Meyer, and P. Morin, J. Electron Spectrosc. Relat. Phenom. **79**, 401 (1996).
[14] J. D. Bozek, N. Saito, and I. H. Suzuki, J. Chem. Phys. **98**, 4652 (1993).
[15] D. Y. Kim, K. Lee, C. I. Ma, M. Mahalingam, D. M. Hanson, and S. L. Hulbuert, J. Chem. Phys. **97**, 5915 (1992).
[16] K. Ueda, K. Ohmori, M. Okunishi, H. Chiba, Y. Shimizu, Y. Sato, T. Hayaishi, E. Shigemasa, and A. Yagishita, Phys. Rev. A **52**, R1815 (1995).
[17] K. Ueda, K. Ohmori, M. Okunishi, H. Chiba, Y. Shimizu, Y. Sato, T. Hayaishi, A. Yagishita, and E. Shigemasa, J. Electron Spectrosc. Relat. Phenom. **79**, 411 (1996).
[18] J. D. Bozek, N. Saito, and I. H. Suzuki, Phys. Rev. A **51**, 4563 (1995).
[19] J. Adachi, N. Kosugi, E. Shigemasa, and A. Yagishita, J. Chem. Phys. **102**, 7369 (1995).
[20] J. Adachi, N. Kosugi, E. Shigemasa, and A. Yagishita, J. Chem. Phys. **107**, 4919 (1997).
[21] Y. Shimizu, K. Ueda, H. Chiba, K. Ohomori, M. Okunishi, Y. Sato, and T. Hayaishi, J. Chem. Phys. **107**, 2415 (1997); Y. Shimizu, K. Ueda, H. Chiba, M. Okunishi, K. Ohomori, J. B. West, Y. Sato, and T. Hayaishi, *ibid.* **107**, 2419 (1997).
[22] K. Ueda, Y. Shimizu, K. Nagao, H. Chiba, M. Okunishi, K. Ohmori, J. B. West, Y. Sato, T. Hayaishi, H. Nakamatsu, and T. Mukoyama, Phys. Rev. Lett. **79**, 3371 (1997).
[23] M. N. Piancastelli, A. Kivimaki, B. Kempgens, M. Neeb, K. Maier, and A. M. Bradshaw, Chem. Phys. Lett. **274**, 13 (1997).
[24] K. C. Prince, L. Avaldi, M. Coreno, R. Camillon, and M. de Simone, J. Phys. B **32**, 2551 (1999).
[25] A. Cesar, F. Gel'mukhanov, Yi Luo, H. Agren, P. Skytt, P Glans, J. Guo, K. Gunnelin, and J. Nordgren, J. Chem. Phys. **106**, 3439 (1997).
[26] S. Tanaka, Y. Kayanuma, and K. Ueda, Phys. Rev. A **57**, 3437 (1998).
[27] H. Köppel, W. Domcke, and L. S. Cederbaum, Adv. Chem. Phys. **57**, 59 (1984).
[28] E. Ishiguro, H. Ohashi, Li-jun Lu, W. Watari, M. Kamizato, and T. Ishikawa, J. Electron Spectrosc. Relat. Phenom. **101-103**, 979 (1999).
[29] H. Ohashi, SPring-8 Information **3(5)**, 12 (1998) (in Japanese).
[30] T. Tanaka and H. Kitamura, Nucl. Instrum. Methods, Phys. Res. A **364**, 368 (1995).
[31] I. Koyano, M. Okuyama, E. Ishiguro, A. Hiraya, H. Ohashi, T. Kanashima, K. Ueda, I. H. Suzuki, and T. Ibuki, J. Synchrotron Radiat. **5**, 545 (1998).
[32] A. Hiraya, Y. Senba, H. Yoshida, and K. Tanaka, J. Electron Spectrosc. Relat. Phenom. **101-103**, 1025 (1999).
[33] J. Adachi, Y. Takata, E. Shigemasa, N. Kosugi, and A. Yagishita, Photon Factory Activity Rep. **16**, 8 (1999).
[34] G. R. Wight and C. E. Brion, J. Electron Spectrosc. Relat. Phenom. **3**, 191 (1974).
[35] K. Nagai, C. Yamada, Y. Endo, and E. Hirota, J. Mol. Spectrosc. **90**, 249 (1981).
[36] R. N. Zare, Mol. Photochem. **4**, 1 (1972).
[37] G. E. Busch and K. R. Wilson, J. Chem. Phys. **56**, 3638 (1972).
[38] J. L. Dehmer and D. Dill, Phys. Rev. A **18**, 164 (1978).
[39] The figure of 20% has been estimated as follows. The intensity ratio of the O $1s\sigma_u^{-1}3s\sigma_g\ \Sigma_u$ resonance in the $I(90°)$ spectrum to the O $1s\sigma_u^{-1}2\pi_u\ \Pi_g$ resonance in the $I(90°)$ spectrum is obtained to be 0.126, which yields that about 20% intensity of the O $1s\sigma_u^{-1}2\pi_u\ \Pi_g$ state produces the O $1s\sigma_u^{-1}3s\sigma_g\ \Sigma_u$ by the quasi-Jahn-Teller coupling.